



HHS Public Access

Author manuscript

JAMA Otolaryngol Head Neck Surg. Author manuscript; available in PMC 2024 September 25.

Published in final edited form as:

JAMA Otolaryngol Head Neck Surg. 2024 July 01; 150(7): 628–630. doi:10.1001/jamaoto.2024.1129.

First-in-Human Hyperpolarized MRI for Tumor Metabolism in HNSCC

Stephen Y. Lai, MD, PhD,

Department of Head and Neck Surgery, The University of Texas MD Anderson Cancer Center, Houston

Vlad C. Sandulache, MD, PhD,

Bobby R. Alford Department of Otolaryngology Head and Neck Surgery, Baylor College of Medicine, Houston, Texas

Dawid Schellingerhout, MBChB,

Department of Diagnostic Imaging, The University of Texas MD Anderson Cancer Center, Houston

Clifton D. Fuller, MD, PhD,

Department of Radiation Oncology, The University of Texas MD Anderson Cancer Center, Houston

Yunyun Chen, PhD,

Department of Head and Neck Surgery, The University of Texas MD Anderson Cancer Center, Houston

Christopher M. Walker, PhD,

Department of Imaging Physics, The University of Texas MD Anderson Cancer Center, Houston

James A. Bankson, PhD

Department of Imaging Physics, The University of Texas MD Anderson Cancer Center, Houston

Metabolic reprogramming has been defined as a hallmark of cancer biology for more than half a century. We and others have identified metabolic shifts in energy and biomass production as intricately linked and causative for both aggressive tumor biology and

Corresponding Authors: Stephen Y. Lai, MD, PhD (sylai@mdanderson.org), and James A. Bankson, PhD (jbankson@mdanderson.org), The University of Texas MD Anderson Cancer Center, 1515 Holcombe Blvd, Unit 1445, Houston, TX 77030.

Additional Contributions: We appreciate the efforts and dedication of personnel in the Center for Advanced Biomedical Imaging and Cyclotron and Radiochemistry Facility within the University of Texas MD Anderson Cancer Center, Houston, including Brandy Reed, MBA, RT(R)(MR), Stephanie Carlon, BSRS, RT(R)(MR)(CT), Michelle Underwood, BSRS, RT(R)(MR)(CT), MRSO, Stacy Hash, RT(R)(MR)(CT), Jerell Jones, BSPH, RT(R)(MR)(CT), MRSO, Freddy Gonzalez, MBA, ARRT(N) NMTCB(CT) PET, Sandra Schuster, BSRS, RT(R)(MR), Andrew Day, PharmD, and Moin Cahriwala, BSN, MS, RN. We highlight the patient care team, including Ehab Y. Hanna, MD, William H. Morrison, MD, and Luana Guimaraes de Sousa, MD, as well as contributions from Keith Michel, PhD. None of the contributors were compensated outside normal salary.

Conflict of Interest Disclosures: Dr Lai has consulted for Cardinal Health. Dr Sandulache has consulted for FemtovoX. Dr Fuller reported grants from the National Cancer Institute; grants, personal fees, and nonfinancial support from Elekta; and travel support from Siemens Healthineers/Varian and Phillips Medical Systems. Dr Bankson reported grants from the National Cancer Institute and GE Healthcare as well as personal fees from NVision Imaging Technologies. No other disclosures were reported.

Disclaimer: The content of this article is solely the responsibility of the authors and does not necessarily represent the views of the National Cancer Institute of the National Institutes of Health.

reduced treatment response in head and neck squamous cell carcinoma (HNSCC).¹ These shifts represent a potentially paradigm-shifting biomarker predictive of treatment response if interrogated with the appropriate spatial and temporal resolution required for clinical translation. Magnetic resonance imaging (MRI) of hyperpolarized pyruvate has been advanced to the threshold of clinical implementation due to its ability to detect shifts in intratumoral metabolic flux, which correlate with oncologic outcomes in preclinical models of HNSCC.^{2,3} Here, we deploy, to our knowledge, hyperpolarized MRI (HP-MRI) of carbon 13 (¹³C) pyruvate in a patient with HNSCC for the first time to demonstrate its translational viability.

Report of a Case |

An adult man with a T2N2M0 human papillomavirus–associated oropharyngeal squamous cell carcinoma was recruited to a prospective imaging registry study at the University of Texas MD Anderson Cancer Center following institutional review board and investigational new drug approval. Imaging was performed prior to treatment initiation; test-retest fidelity was assessed via serial tracer injection and scanning 40 minutes apart. Briefly, 250-millimolar hyperpolarized [¹⁻¹³C] pyruvate was prepared using a SpinLab dissolution dynamic nuclear polarization system (Research Circle Technology). Imaging data were acquired on a 3-T MR750 MRI scanner (GE Healthcare). Anatomic MRI to confirm positioning and localize the tumor was carried out using the ¹H body coil. Metabolic imaging data were acquired using a Helmholtz clamshell transmit coil for ¹³C excitation and a pair of 4-element paddle arrays placed on either side of the patient’s head for detection of hyperpolarized ¹³C signal. Dynamic HP-MRI data were acquired using a broad-band echo planar imaging sequence with spatially and spectrally selective excitation pulses. A constant excitation scheme (nominal pyruvate $\theta = 20^\circ$; lactate $\theta = 30^\circ$)⁴ was used to excite eight 1.5 cm–thick slices that were encoded over a 24 × 24 cm field of view with a 16 × 16 image matrix to provide 1.5 cm in-plane resolution every 3 seconds for a total of 3 minutes, beginning just prior to intravenous bolus administration of hyperpolarized pyruvate (0.43 mL/kg). Dynamic data were analyzed on a voxel-by-voxel basis by integrating the area under the dynamic signal curve (AUC) for pyruvate and lactate, calculating the ratio of lactate to the sum of pyruvate and lactate, and fitting to pharmacokinetic models that we have previously described and made publicly available.⁵ Data were analyzed using Matlab version R2021b (Mathworks).

The patient successfully underwent imaging, which allowed for measurement of pyruvate and lactate AUC in both the primary tumor and associated nodal basins (Figure 1). Spatial resolution permitted separation of normalized lactate values from the primary tumor and bilateral cervical metastases (Figure 2). Serial delivery of the tracer and imaging demonstrated strong correlation between repeated measurements in regions of disease ($\rho = 0.97$; $P < .001$). The patient tolerated the procedure without complications.

Discussion |

HP-MRI is a minimally invasive and well-tolerated means of assessing intratumoral metabolic shifts, with spatial resolution on the order of a centimeter. Promising test-retest

reproducibility indicates significant potential for clinical translation. These characteristics make it ideally suited for longitudinal observations and development of adaptive treatment strategies for HNSCC, particularly those with a spatial component (eg, external beam radiation). Continued development of HP-MRI is necessary to define tumor heterogeneity in response to both targeted and systemic therapies to drive adaptive modification of a comprehensive treatment plan for both primary tumor and associated locoregional metastases. Future studies at our site will test the feasibility of HP-MRI deployment at scale in patients with HNSCC prior to and during treatment as the next stage of biomarker development.

Funding/Support:

This work was supported in part through funding from the National Cancer Institute of the National Institutes of Health (R01CA211150, R01CA280980, and U54CA274321) and GE Healthcare.

Role of the Funder/Sponsor:

The funders had no role in the design and conduct of the study; collection, management, analysis, and interpretation of the data; preparation, review, or approval of the manuscript; and decision to submit the manuscript for publication.

References

1. Yu W, Chen Y, Putluri N, et al. Evolution of cisplatin resistance through coordinated metabolic reprogramming of the cellular reductive state. *Br J Cancer*. 2023;128(11):2013–2024. doi:10.1038/s41416-023-02253-7 [PubMed: 37012319]
2. Chen Y, Maniakas A, Tan L, et al. Development of a rational strategy for integration of lactate dehydrogenase A suppression into therapeutic algorithms for head and neck cancer. *Br J Cancer*. 2021;124(10):1670–1679. doi:10.1038/s41416-021-01297-x [PubMed: 33742144]
3. Sandulache VC, Chen Y, Lee J, et al. Evaluation of hyperpolarized [1-¹³C]-pyruvate by magnetic resonance to detect ionizing radiation effects in real time. *PLoS One*. 2014;9(1):e87031. doi:10.1371/journal.pone.0087031 [PubMed: 24475215]
4. Walker CM, Fuentes D, Larson PEZ, Kundra V, Vigneron DB, Bankson JA. Effects of excitation angle strategy on quantitative analysis of hyperpolarized pyruvate. *Magn Reson Med*. 2019;81(6):3754–3762. doi:10.1002/mrm.27687 [PubMed: 30793791]
5. Bankson JA, Walker CM, Ramirez MS, et al. Kinetic modeling and constrained reconstruction of hyperpolarized [1-¹³C]-pyruvate offers improved metabolic imaging of tumors. *Cancer Res*. 2015;75(22):4708–4717. doi:10.1158/0008-5472.CAN-15-0171 [PubMed: 26420214]
6. Lai S Data from: Supplementary figures - HP-MRI first in human HNSCC.pdf. figshare. 2024. doi:10.6084/m9.figshare.25497505.v1

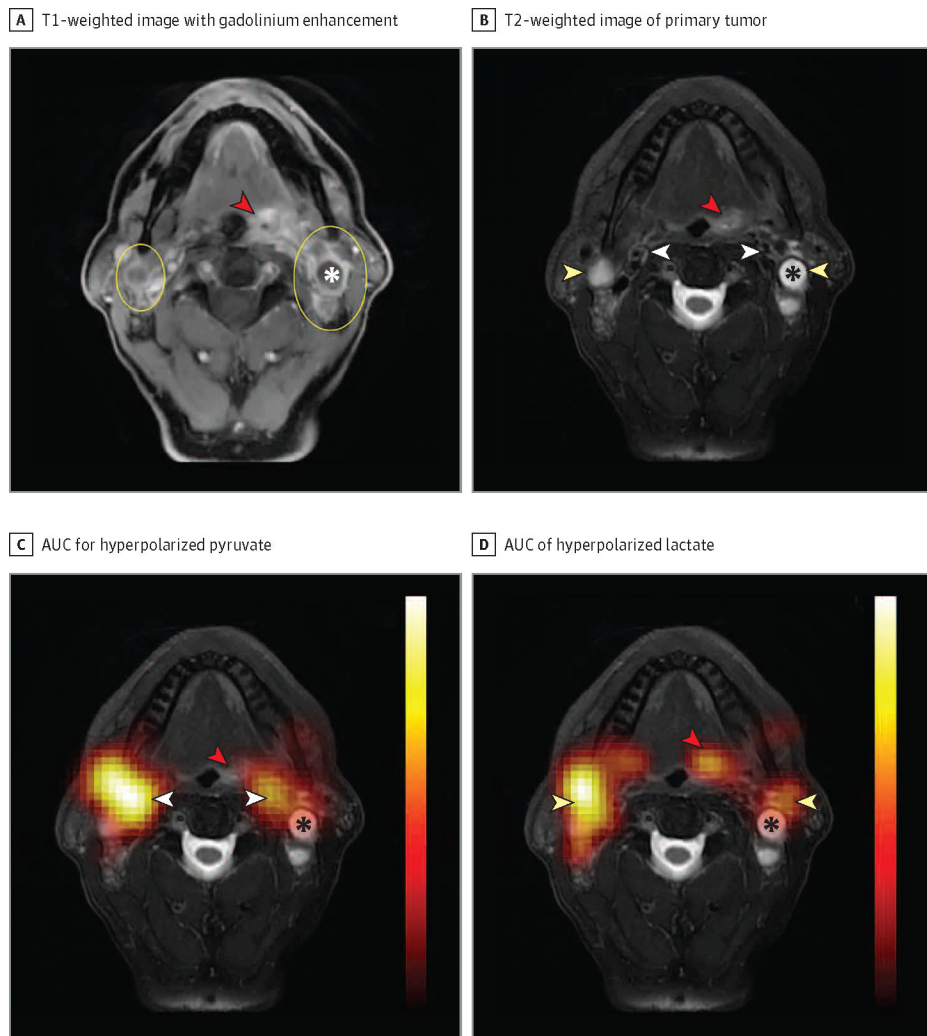


Figure 1. Tongue Base Carcinoma With Bilateral Upper Neck Lymphadenopathy

A, T1-weighted image with gadolinium enhancement showing the primary tumor (red arrowhead) and bilateral neck lymphadenopathy (yellow ovals). B, The primary tumor (red arrowhead) and bilateral metastatic lymph nodes (yellow arrowheads) are again indicated on T2-weighted images. We also show the vasculature (white arrowheads) anteromedial to the metastatic lymph nodes. C, Area under the dynamic signal curve (AUC) measurements for hyperpolarized pyruvate superimposed over the T2-weighted anatomic reference shows pyruvate signal to strongly localize over the vasculature (white arrowheads), with relatively little pyruvate signal over the primary tumor (red arrowhead) and metastatic lymph nodes. D, AUC of hyperpolarized lactate superimposed on the T2-weighted anatomic reference shows strong localization of the lactate over the metastatic lymph nodes (yellow arrowheads) with decreased signal over the vasculature and strong signal over the primary tumor (red arrowhead). The apparent shift in signal from the vasculature on pyruvate images to the lymph nodes and primary tumor on lactate images reflects the conversion of lactate from hyperpolarized pyruvate. Lactate dehydrogenase and other enzymes that mediate this conversion are frequently upregulated in head and neck squamous cell carcinoma and in many other cancers. Note the relative paucity of lactate signal over the major necrotic

portion of the left-sided neck lymph node (asterisk). In the absence of enzymes in necrotic tissue, no conversion takes place. Hyperpolarized overlays (1.5-cm thickness and resolution) are interpolated for display. Additional anatomic reference images that overlap with the hyperpolarized magnetic resonance imaging slice and dynamic signal series are available.⁶

Author Manuscript

Author Manuscript

Author Manuscript

Author Manuscript

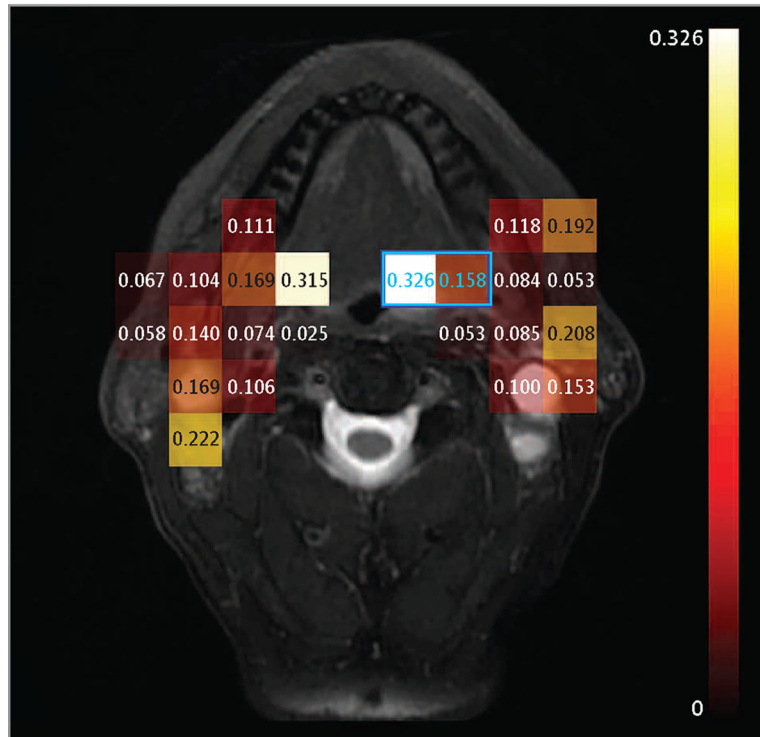
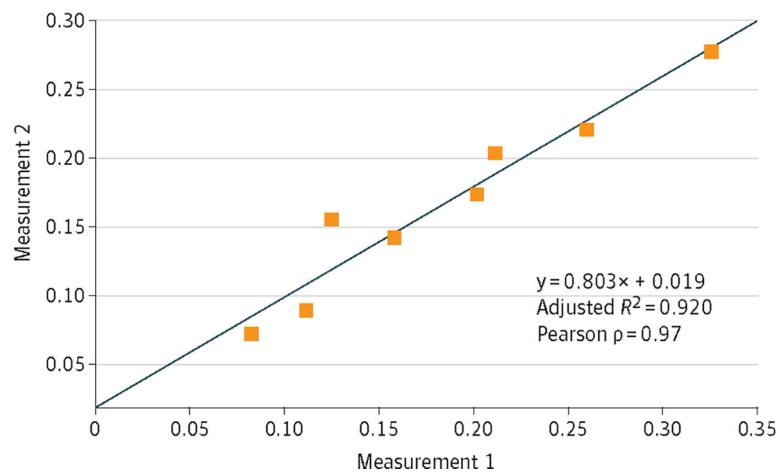
A nLac values**B** Comparison of nLac values

Figure 2. Normalized Lactate Ratio (nLac) as a Reproducible Semiquantitative Imaging Biomarker for Tumor Metabolism

nLac is calculated as the ratio of the area under the dynamic signal curve (AUC) for lactate to the AUC of the total hyperpolarized carbon 13 signal (pyruvate plus lactate). A, nLac values are calculated for each voxel in which the total hyperpolarized ^{13}C signal-to-noise ratio exceeds 10:1. B, Comparison of nLac values from serial observations of tumor-containing voxels (at least 30% by cross-section as judged from anatomic images) within a single imaging session but separated by approximately 40 minutes. The Pearson correlation coefficient shows very strong correlation ($\rho = 0.97$; $P < .001$) between repeated

measurements within 8 voxels captured across all slices (2 such voxels are indicated by blue outline and values). While the line of identity is within the confidence intervals of this regression, further study is warranted to determine if a slope of less than unity reflects a transient saturation of pyruvate uptake or metabolism.